

SUPPLEMENTARY FIGURES

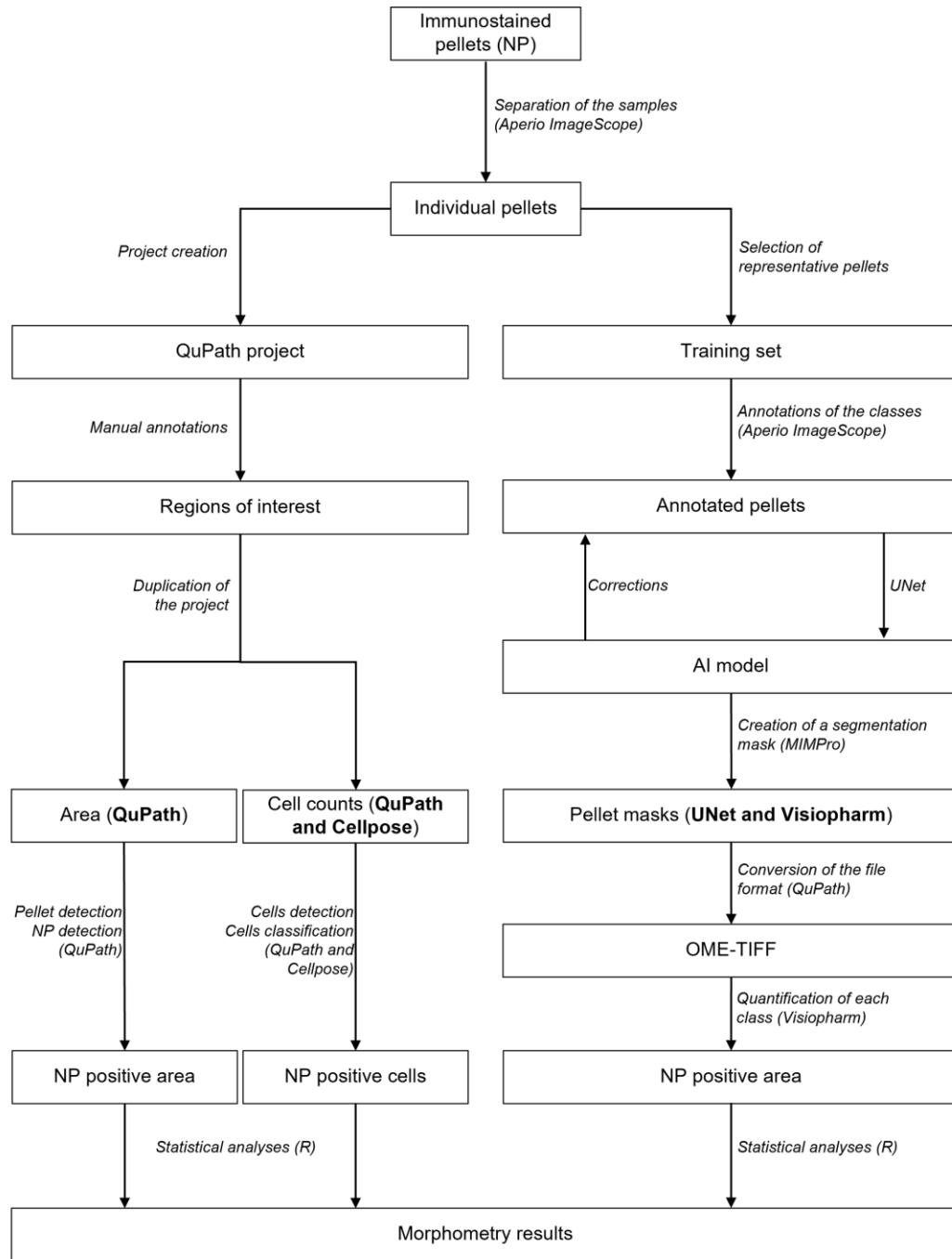


Figure S1. Overview of the image analysis workflow used for the morphometric analyses performed on UGV-1 infected I/IKi cell pellet sections immunostained for reparamavirus nucleoprotein (NP). Digital analyses were performed on the immunostained cell pellets using three different approaches, namely: QuPath (NP positive area), QuPath and Cellpose (NP positive cells), and UNet with Visiopharm (NP positive area). The output of each method was used to calculate the percentage of either NP positive area or NP positive cells per section. Abbreviations: AI: Artificial Intelligence.

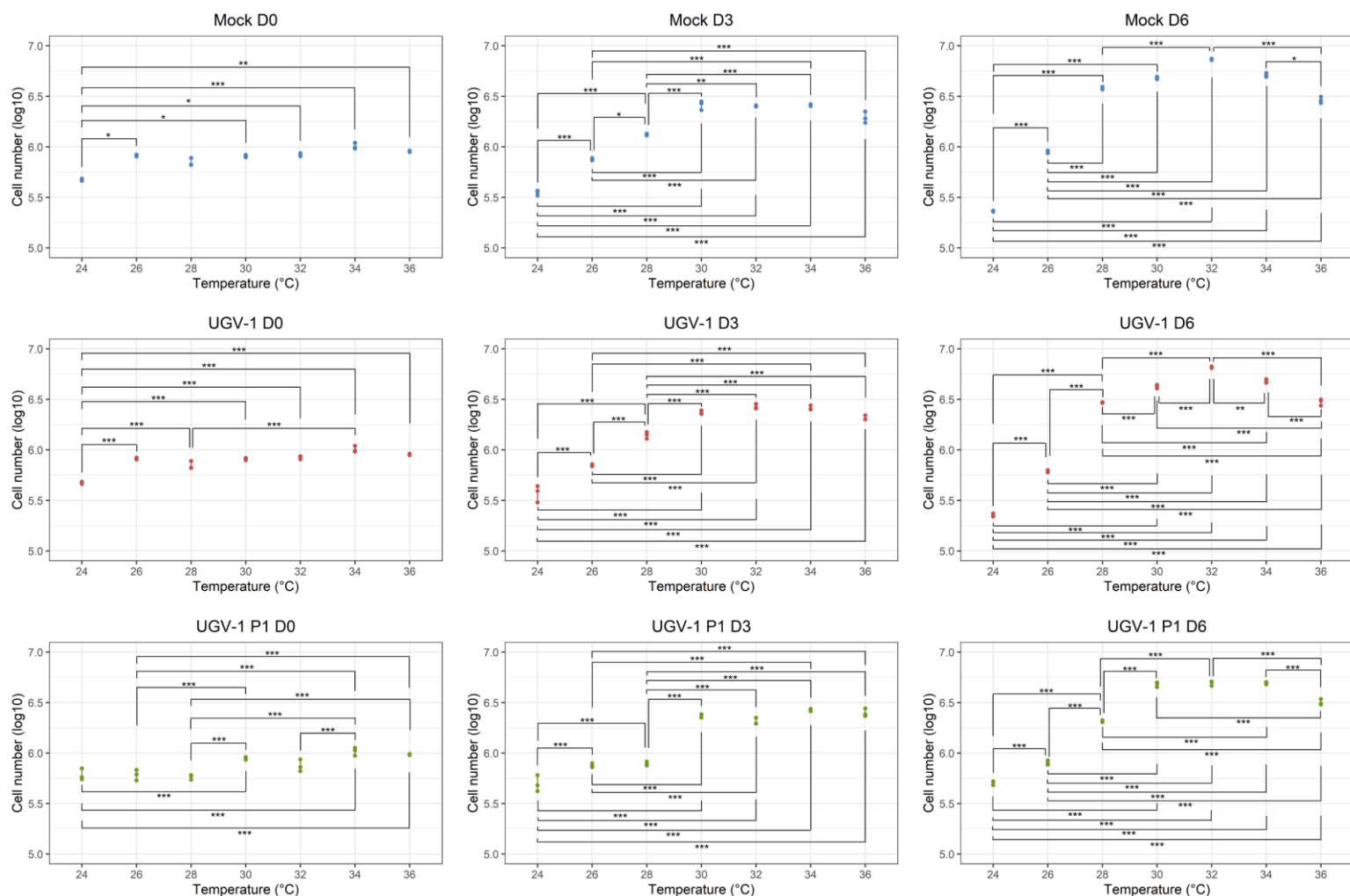


Figure S2. Statistical analyses on growth of mock-infected and freshly or passed reptarenavirus-infected I/1Ki cells comparing different temperatures for each timepoint. I/1Ki cells were seeded onto 6-well plates at 7×10^5 cells/well and incubated at different temperatures (24-36°C). The adherent cells/well were counted with a LUNA-II™ Automated Cell Counter at D0 (1 day after seeding) and D3 and D6, after inoculation with UGV-1 at MOI=10 or mock inoculation at D0. In addition, I/1Ki cells at 15 d post UGV-1 inoculation (P1) were plated onto 6 well-plates at equivalent cell density and counted at the corresponding timepoints. We used biological triplicates for each condition. The figure shows scatter plots of the cell numbers (Y-axis, logarithmic scale) at the different temperatures (X-axis). The graphs depict the statistical significant differences on cell counts among different temperatures: *: $0.05 \geq p\text{-value} > 0.01$; **: $0.01 \geq p\text{-value} > 0.001$; ***: $p\text{-value} < 0.001$. The raw data are provided in Table S1. The statistical analyses are also presented in Table S2.

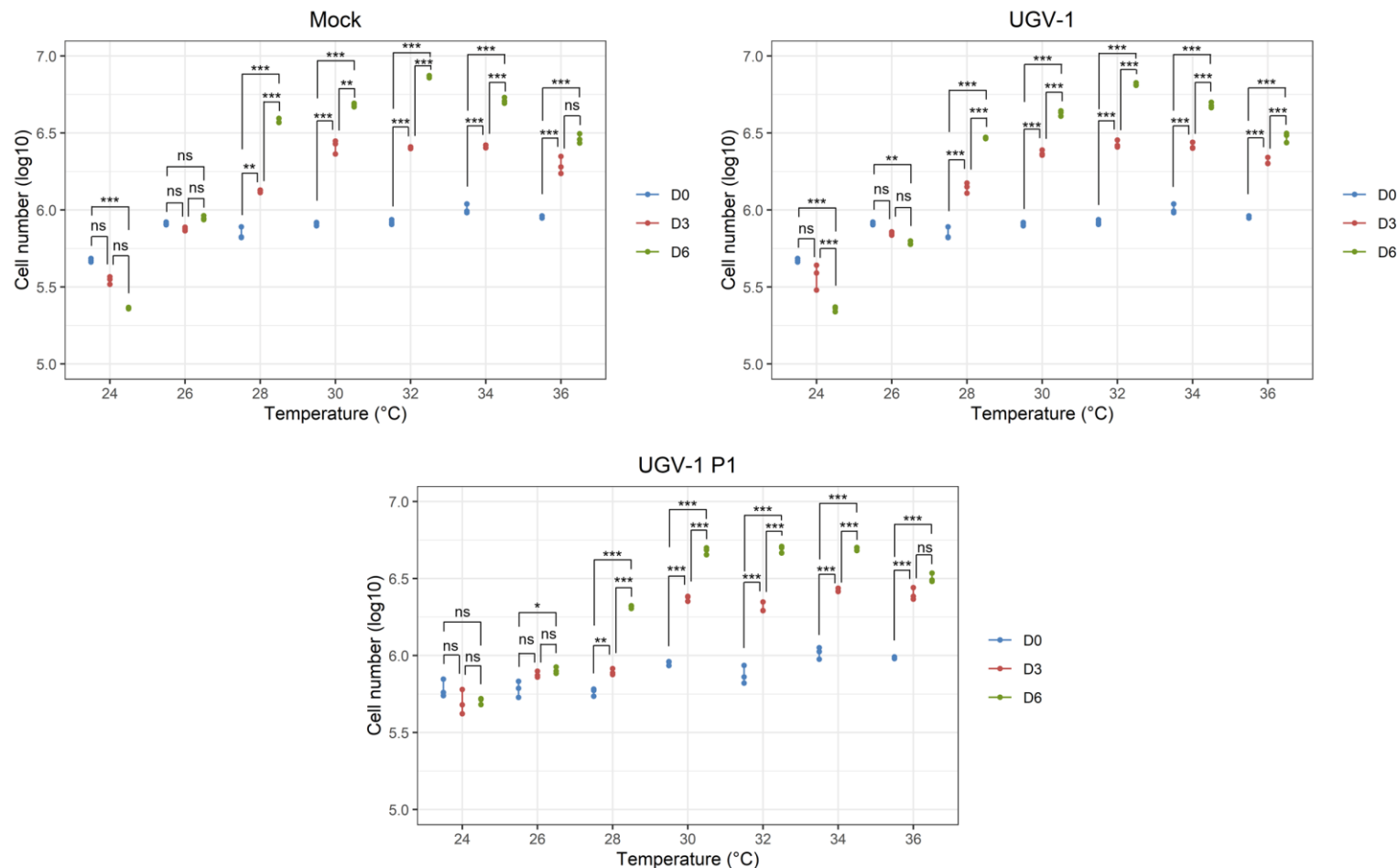


Figure S3. Statistical analyses on growth of mock-infected and freshly or passaged reptarenavirus-infected I/1Ki cells comparing different timepoints for each temperature. I/1Ki cells were seeded onto 6-well plates at 7×10^5 cells/well and incubated at different temperatures (24-36°C). The adherent cells/well were counted with a LUNA-II™ Automated Cell Counter at D0 (1 day after seeding) and D3 and D6, after inoculation with UGV-1 at MOI=10 or mock inoculation at D0. In addition, I/1Ki cells at 15 d post UGV-1 inoculation (P1) were plated onto 6 well-plates at equivalent cell density and counted at the corresponding timepoints. We used biological triplicates for each condition. The figure shows scatter plots of the cell numbers (Y-axis, logarithmic scale) at the different temperatures and timepoints (X-axis). The graphs depict the statistical significant differences on cell counts among different timepoints for each temperature: *: $0.05 \geq p\text{-value} > 0.01$; **: $0.01 \geq p\text{-value} > 0.001$; ***: $p\text{-value} < 0.001$; ns: not significant. The raw data are provided in Table S1. The statistical analyses are also presented in Table S2.

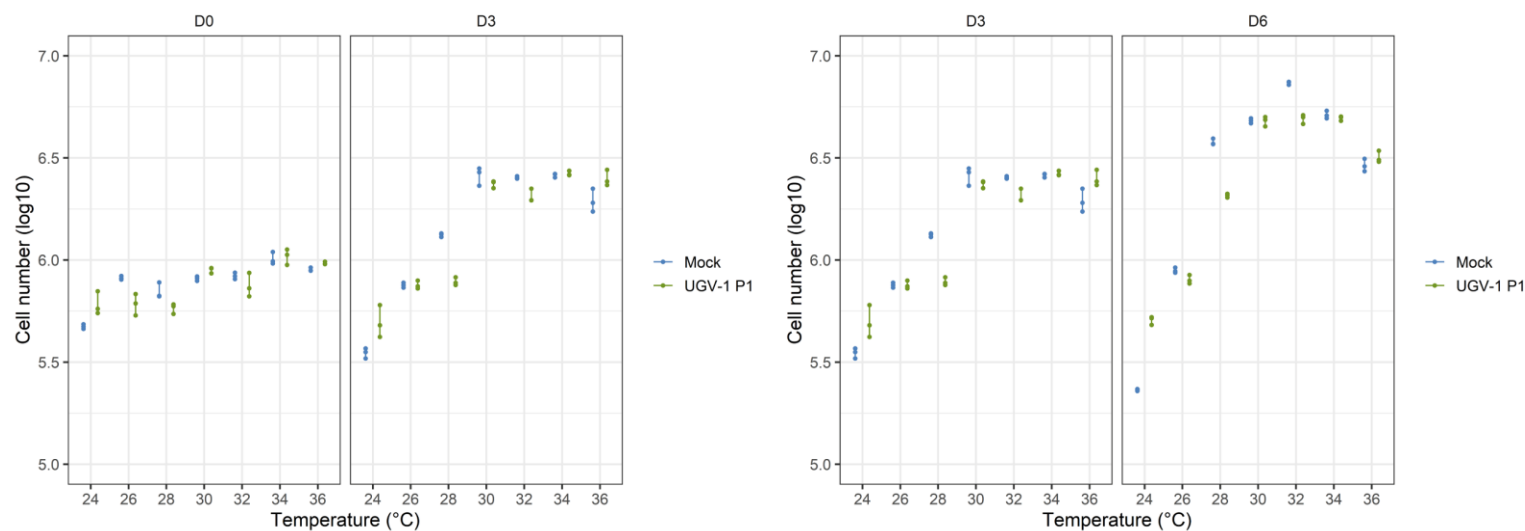


Figure S4. Growth of passaged reptarenavirus-infected I/1Ki cells (UGV-1 P1) in comparison to mock infected cells. I/1Ki cells were seeded onto 6-well plates at 7×10^5 cells/well and incubated at different temperatures (24-36°C). The adherent cells/well were counted with a LUNA-II™ Automated Cell Counter at D0 (1 day after seeding) and D3 and D6, after inoculation with UGV-1 at MOI=10 or mock inoculation at D0. In addition, I/1Ki cells at 15 d post UGV-1 inoculation (P1) were plated onto 6 well-plates at equivalent cell density and counted at the corresponding timepoints. We used biological triplicates for each condition. The figure shows scatter plots of the cell numbers (Y-axis, logarithmic scale) at the different temperatures and timepoints (X-axis): D0 and D3 (left) and D3 and D6 (right). The raw data are provided in Table S1. The statistical analyses are presented in Figures S2, S3 and S5, and Table S2.

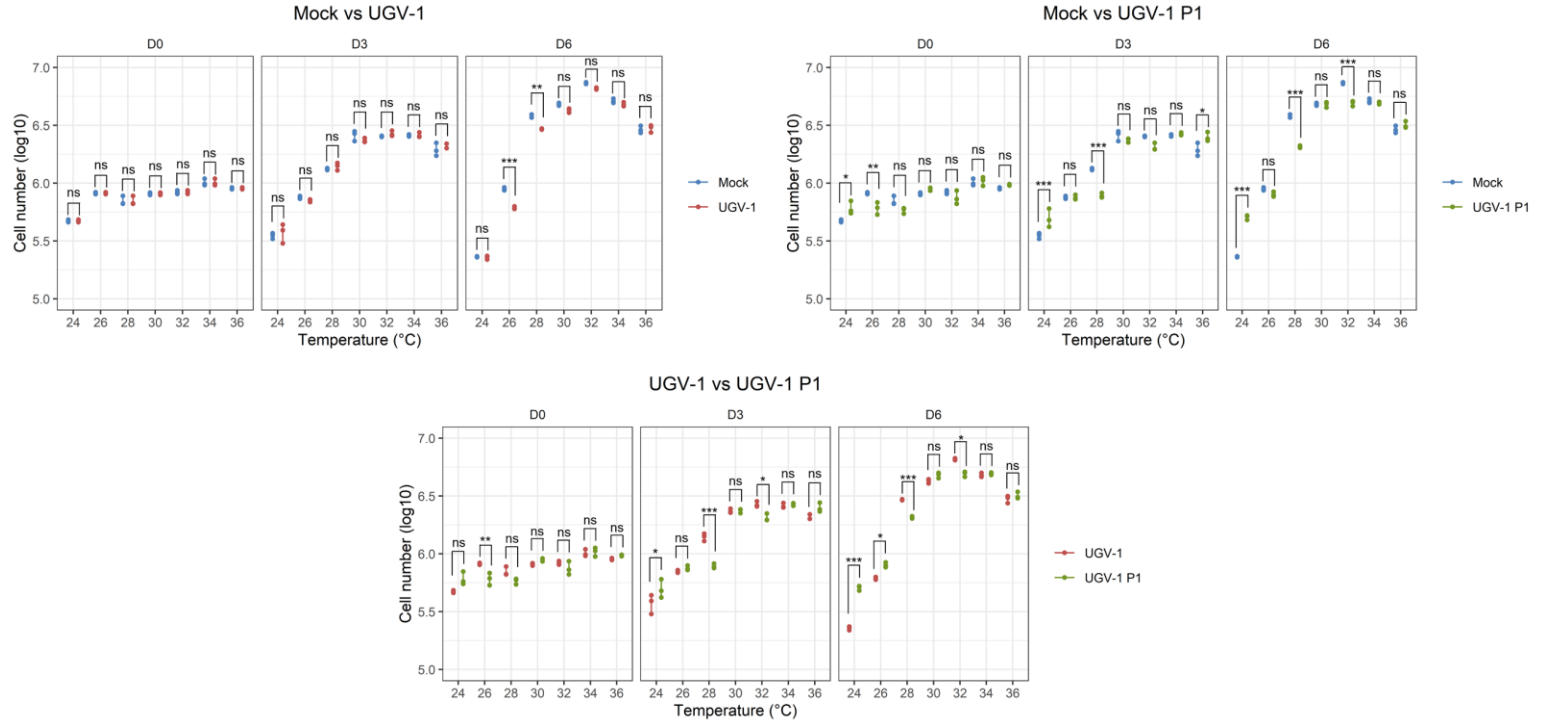


Figure S5. Statistical analyses comparing growth of mock-infected, freshly and passaged reptarenavirus-infected I/1Ki cells for each timepoint and temperature. I/1Ki cells were seeded onto 6-well plates at 7×10^5 cells/well and incubated at different temperatures (24-36°C). The adherent cells/well were counted with a LUNA-II™ Automated Cell Counter at D0 (1 day after seeding) and D3 and D6, after inoculation with UGV-1 at MOI=10 or mock inoculation at D0. In addition, I/1Ki cells at 15 d post UGV-1 inoculation (P1) were plated onto 6 well-plates at equivalent cell density and counted at the corresponding timepoints. We used biological triplicates for each condition. The figure shows scatter plots of the cell numbers (Y-axis, logarithmic scale) at the different temperatures and timepoints (X-axis). The graphs depict the statistical significant differences on cell counts among mock-infected (Mock), freshly infected (UGV-1) and passaged (UGV-1 P1) infected cells: *: $0.05 \geq p\text{-value} > 0.01$; **: $0.01 \geq p\text{-value} > 0.001$; ***: $p\text{-value} < 0.001$; ns: not significant. The raw data are provided in Table S1. The statistical analyses are also presented in Table S2.

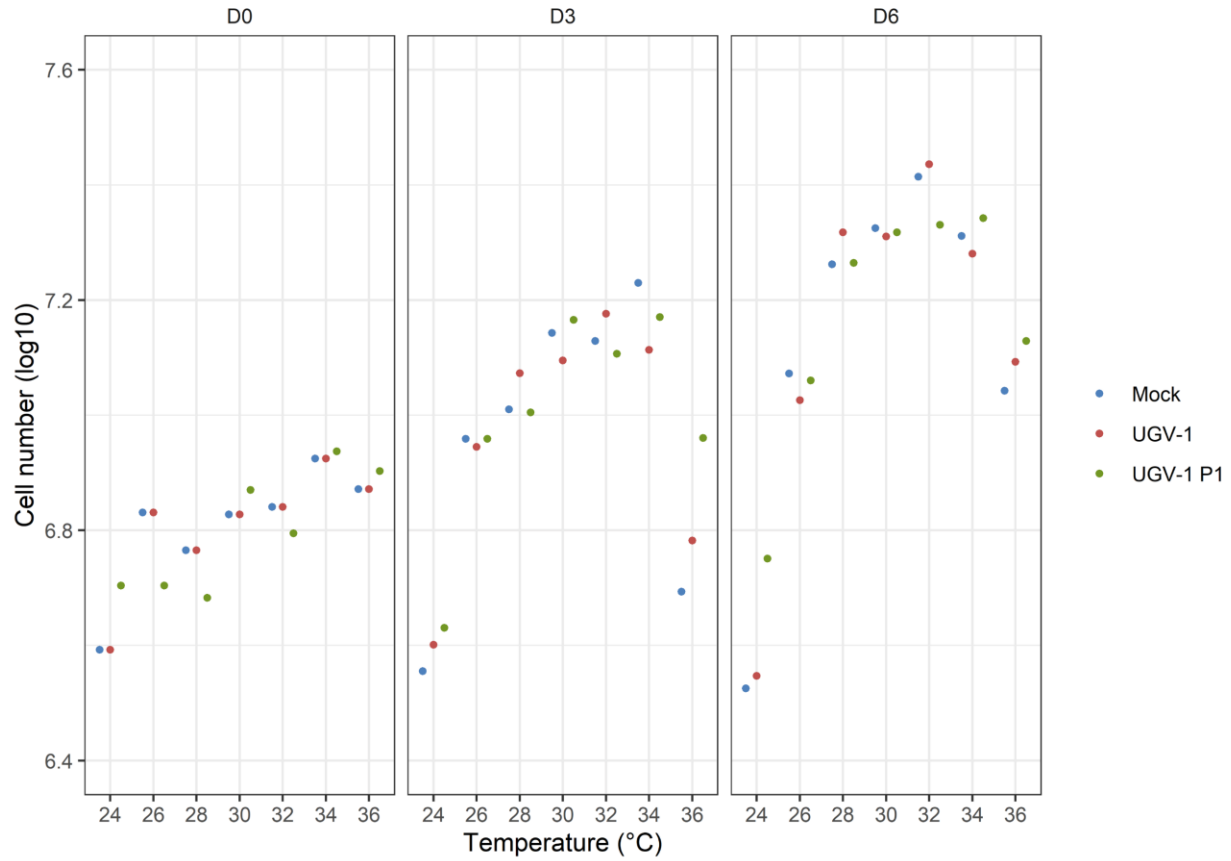


Figure S6. Growth of mock-infected, freshly and passaged reptarenavirus-infected I/1Ki cells plated in flasks. I/1Ki cells were seeded in T75 cm² flasks at 6.2×10^6 cells/flask and incubated at different temperatures (24-36°C). The adherent cells/flasks were counted with a LUNA-II™ Automated Cell Counter at D0 (1 day after seeding) and D3 and D6, after inoculation with UGV-1 at MOI=10 or mock inoculation at D0. In addition, I/1Ki cells at 15 d post UGV-1 inoculation (P1) were plated in T75 cm² flasks at equivalent cell density and counted at the corresponding timepoints. We used a single flask for each condition. The figure shows scatter plots of the cell numbers (Y-axis, logarithmic scale) at the different temperatures and timepoints (X-axis). The raw data are provided in Table S1.

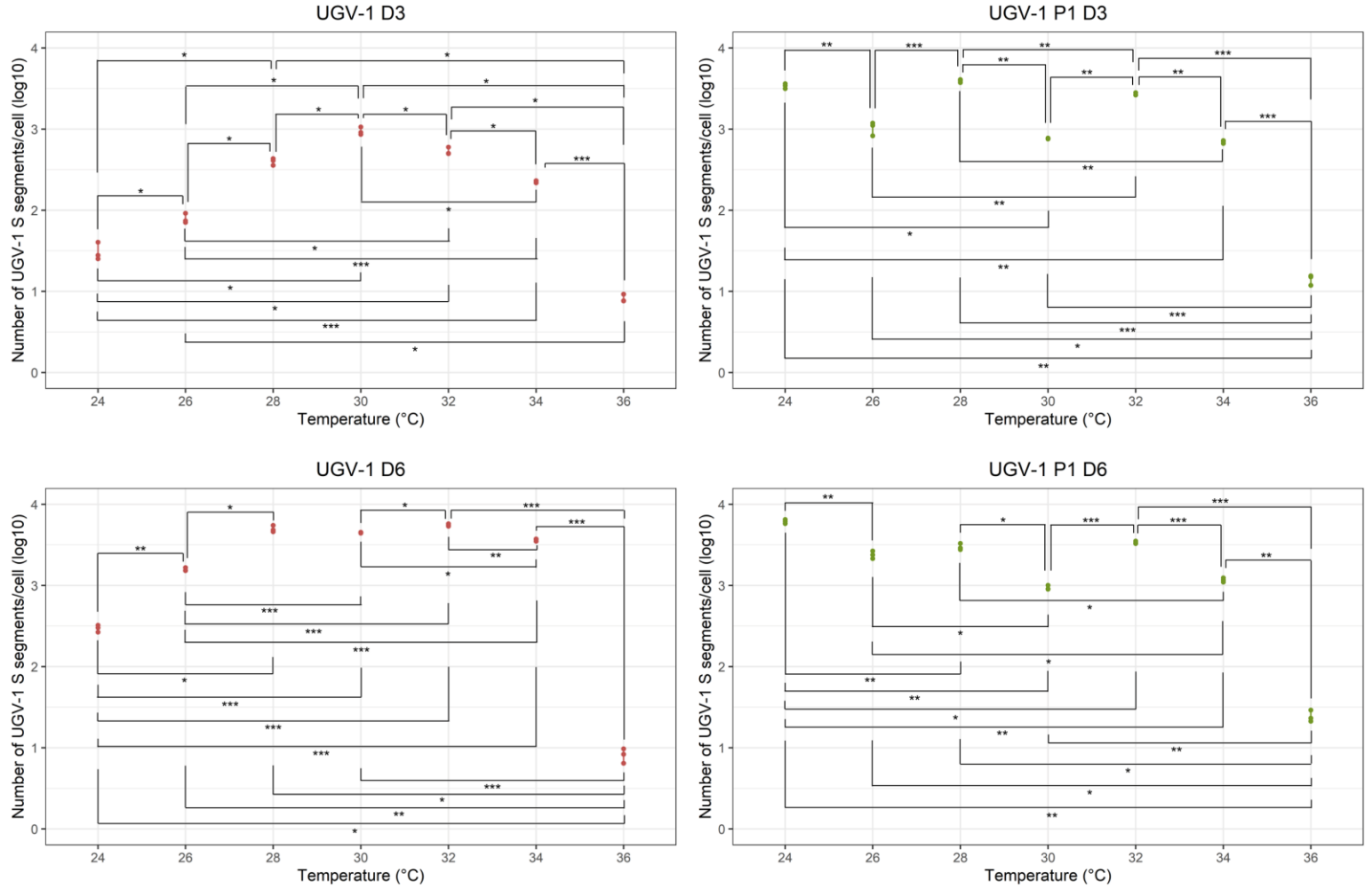


Figure S7. Statistical analyses on viral RNA release per infected I/1Ki cell comparing different temperatures for each timepoint. Viral RNA was isolated from I/1Ki cell culture supernatants collected at D3 and D6 after UGV-1 inoculation at MOI=10 and incubation at 24-36°C, and at the corresponding timepoints after passing I/1Ki cells at 15 d post UGV-1 inoculation (P1). The number of UGV-1 S segments released per cell were quantified through qRT-PCR from biological triplicates for each condition. The figure shows scatter plots of the number (cumulative for D6) of UGV-1 S segments released per cell (Y-axis, logarithmic scale) for freshly UGV-1 inoculated (UGV-1) or passaged cells (UGV-1 P1) at the different temperatures (X-axis). The graphs depict the statistical significant differences on viral RNA released/cell among different temperatures: *: $0.05 \geq p\text{-value} > 0.01$; **: $0.01 \geq p\text{-value} > 0.001$; ***: $p\text{-value} < 0.001$. The raw data are provided in Table S3. The statistical analyses are also in Table S4.

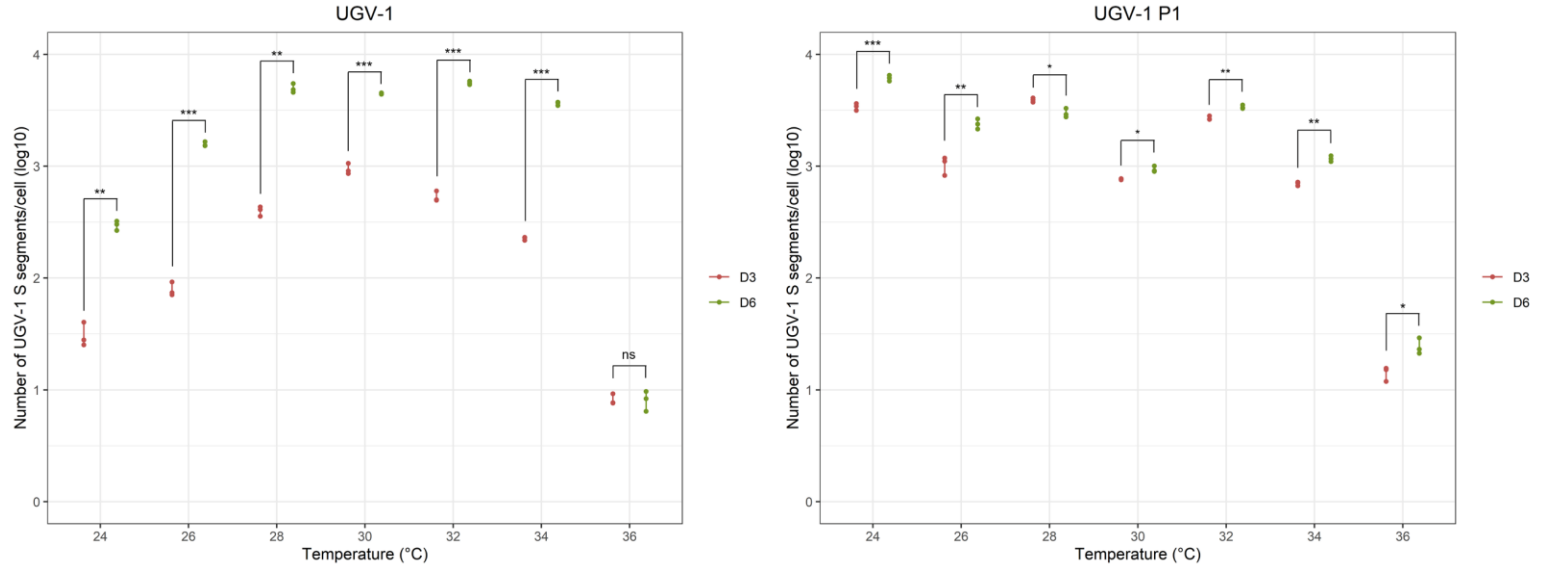


Figure S8. Statistical analyses on viral RNA release per infected I/1Ki cell comparing different timepoints for each temperature. Viral RNA was isolated from I/1Ki cell culture supernatants collected at D3 and D6 after UGV-1 inoculation at MOI=10 and incubation at 24-36°C, and at the corresponding timepoints after passaging I/1Ki cells at 15 d post UGV-1 inoculation (P1). The number of UGV-1 S segments released per cell were quantified through qRT-PCR from biological triplicates for each condition. The figure shows scatter plots of the number (cumulative for D6) of UGV-1 S segments released per cell (Y-axis, logarithmic scale) for freshly UGV-1 inoculated (UGV-1) or passaged (UGV-1 P1) cells at the different temperatures (X-axis). The graphs depict the statistical significant differences on viral RNA released/cell between timepoints for each temperature: *: $0.05 \geq p\text{-value} > 0.01$; **: $0.01 \geq p\text{-value} > 0.001$; ***: $p\text{-value} < 0.001$; ns: not significant. The raw data are provided in Table S3. The statistical analyses are also in Table S4.

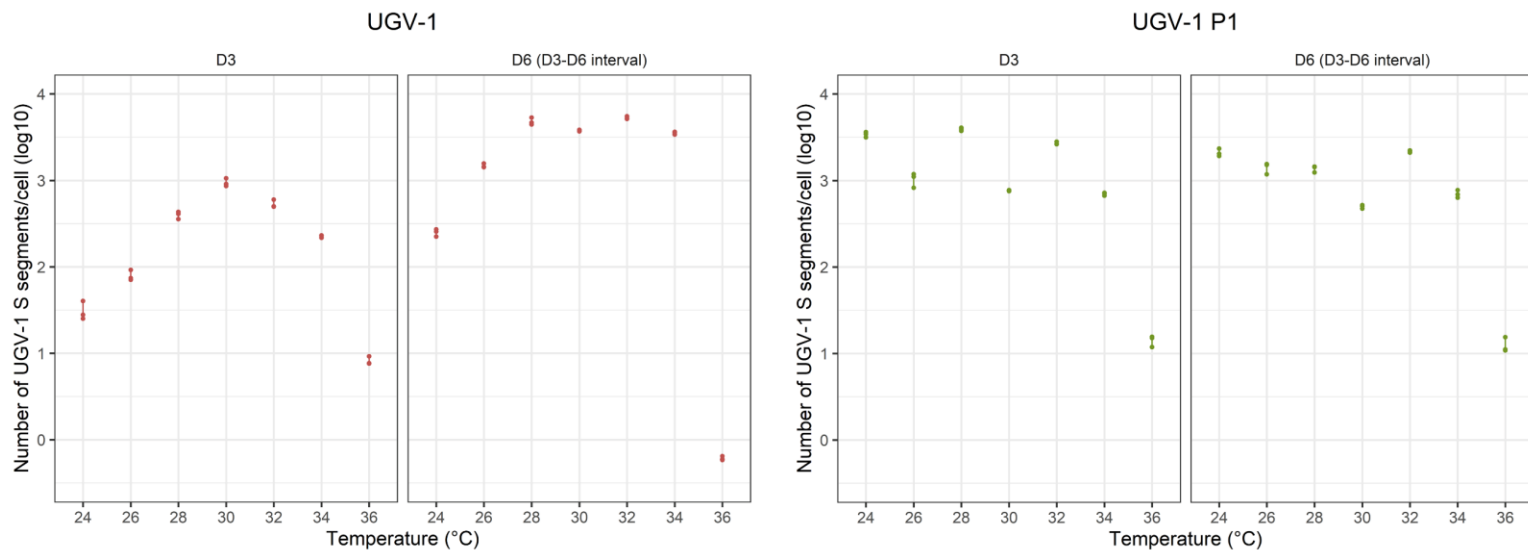


Figure S9. Three-day interval viral RNA release per infected I/1Ki cell. Viral RNA was isolated from I/1Ki cell culture supernatants collected at D3 and D6 after UGV-1 inoculation at MOI=10 and incubation at 24–36°C as well as at the corresponding timepoints after passaging I/1Ki cells at 15 d post UGV-1 inoculation (P1). The number of UGV-1 S segments released per cell was quantified through qRT-PCR from biological triplicates for each condition. The figure shows scatter plots of the number of UGV-1 S segments released per cell (Y-axis, logarithmic scale) for freshly UGV-1 inoculated cells (UGV-1, left) or cells passaged at 15 d post UGV-1 inoculation (UGV-1 P1, right) at the different temperatures and timepoints (X-axis), with D6 representing the 3-day time interval between D3 and D6. The raw data are provided in Table S3. The statistical analyses are presented in Figures S7, S8 and S10, and Table S4.

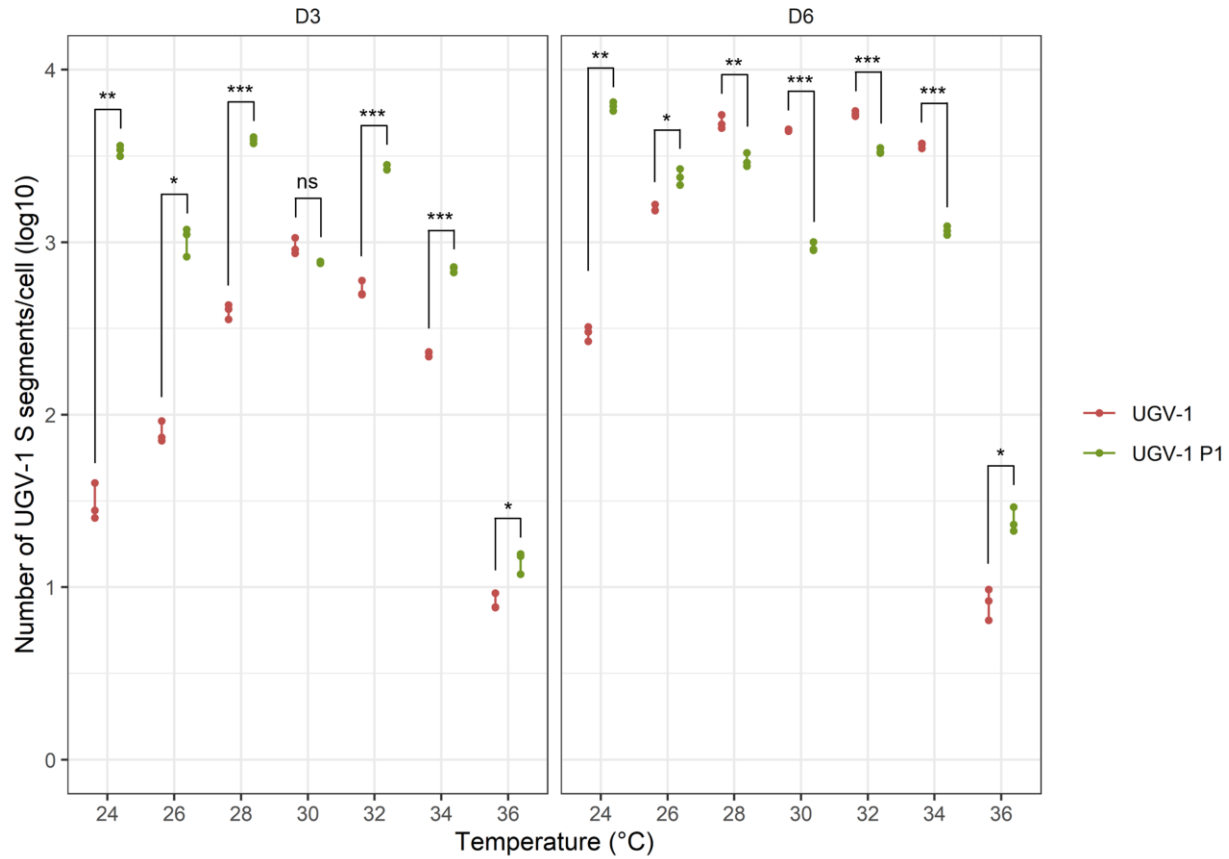


Figure S10. Statistical analyses on viral RNA release per cell comparing freshly and passaged infected I/1Ki cells for each timepoint and temperature. Viral RNA was isolated from I/1Ki cell culture supernatants collected at D3 and D6 after UGV-1 inoculation at MOI=10 and incubation at 24-36°C, and at the corresponding timepoints after passaging I/1Ki cells at 15 d post UGV-1 inoculation (P1). The number of UGV-1 S segments released per cell were quantified through qRT-PCR from biological triplicates for each condition. The figure shows scatter plots of the number (cumulative for D6) of UGV-1 S segments released per cell (Y-axis, logarithmic scale) for freshly UGV-1 inoculated (UGV-1) or passaged (UGV-1 P1) cells at the different temperatures and timepoints (X-axis). The graphs depict the statistical significant differences on viral RNA released/cell between freshly and passaged infected cells: *: $0.05 \geq p\text{-value} > 0.01$; **: $0.01 \geq p\text{-value} > 0.001$; ***: $p\text{-value} < 0.001$; ns: not significant. The raw data are provided in Table S3. The statistical analyses are also in Table S4.

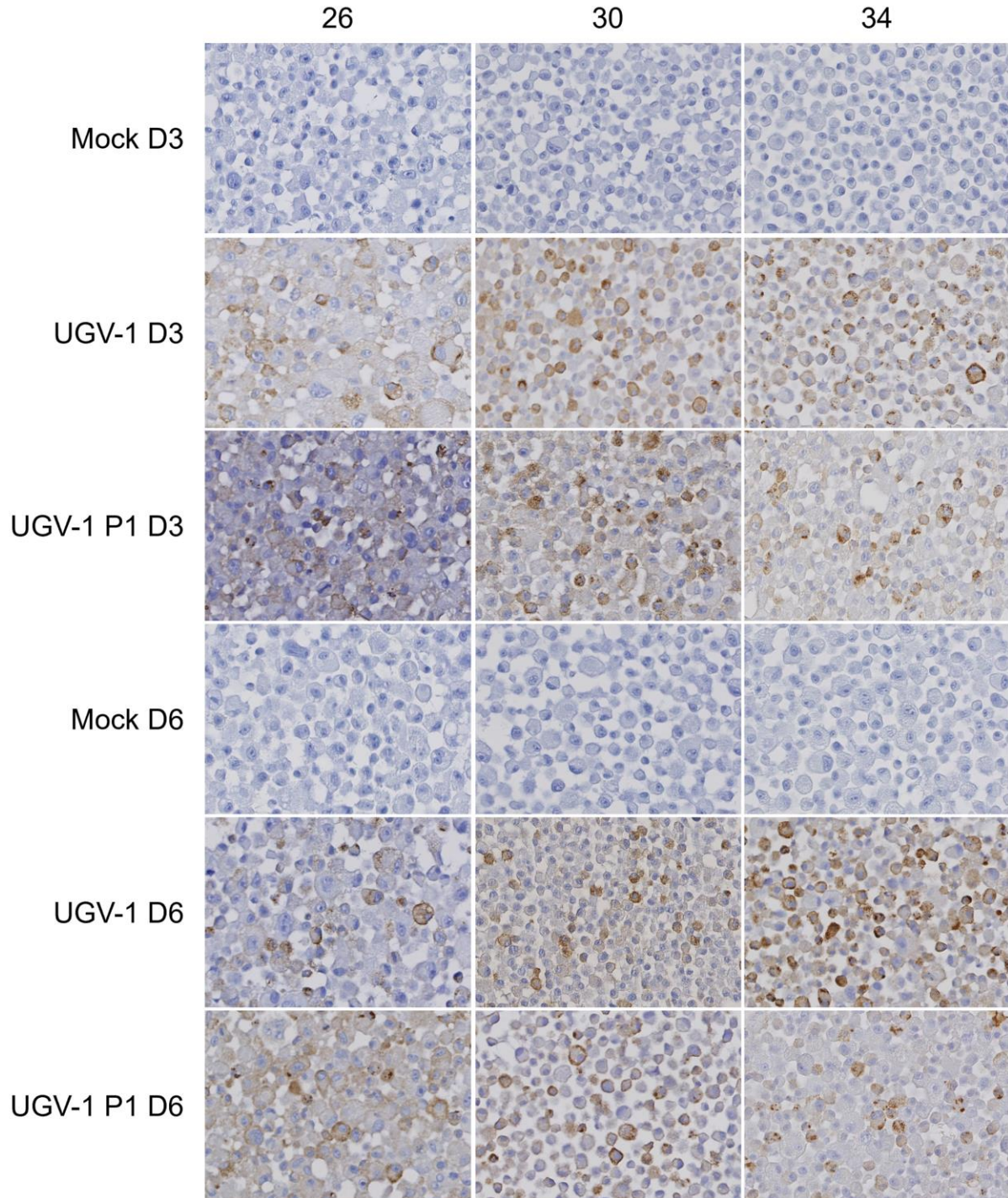


Figure S11. Illustration of viral NP expression in I/1Ki cells infected with UGV-1. Cell pellets were prepared, formalin-fixed and paraffin-embedded. For each pellet, 10 consecutive sections were immunostained using a rabbit antiserum raised against reptarenavirus NP and DAB as chromogen, with haematoxylin counterstain. This figure illustrates the reaction pattern and extent in freshly UGV-1 inoculated cells or cells passaged at 15 d post UGV-1 inoculation (P1) and incubated at 26, 30 or 34°C, at D3 or D6. Mock-infected cells, stained at the same timepoints, serve as negative controls; they do not show any reaction.

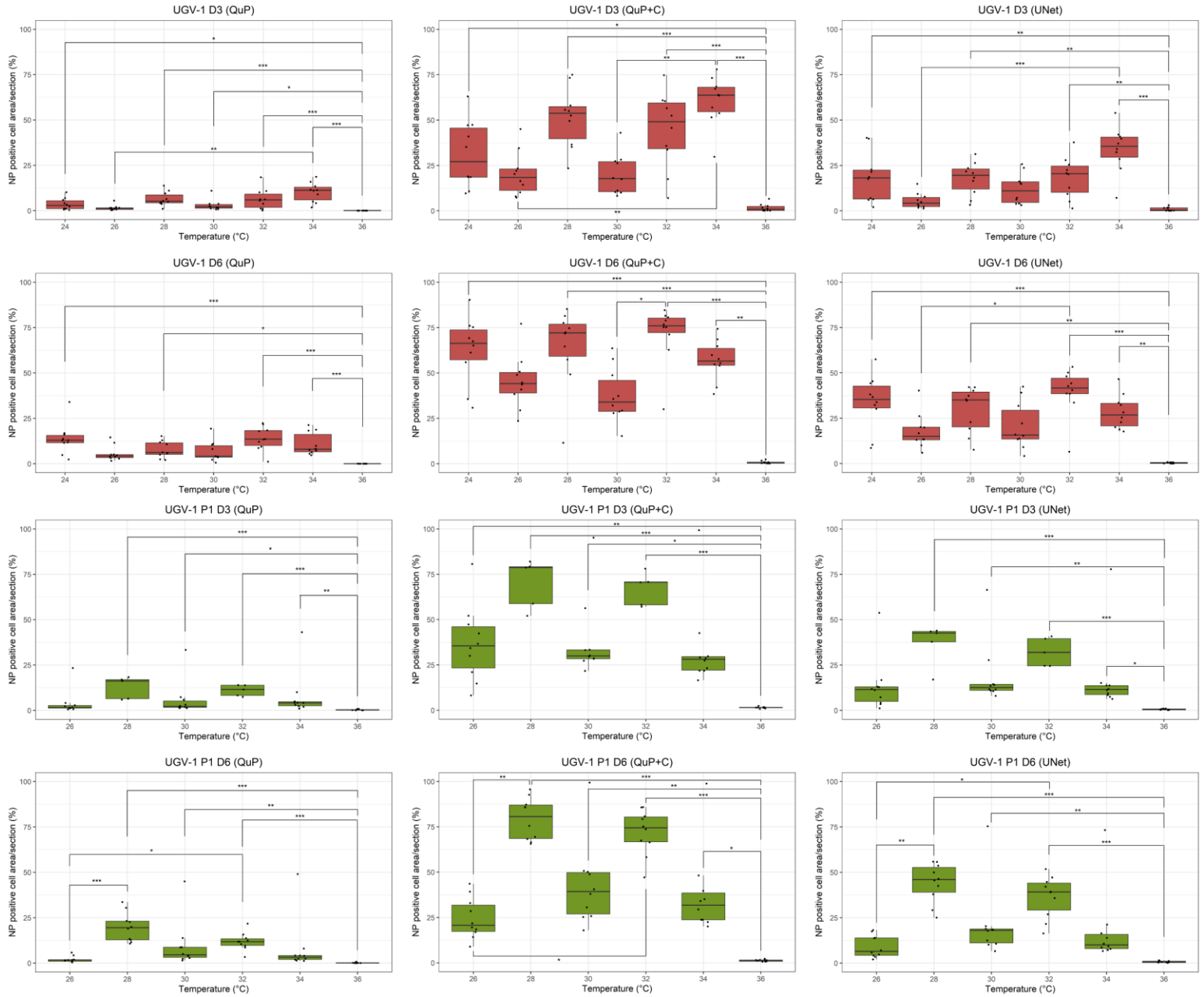


Figure S12. Statistical analyses on the quantification of NP expression in I/1Ki cells infected with UGV-1 comparing different temperatures for each timepoint. Cell pellets were prepared, formalin-fixed and paraffin-embedded. For each pellet, 10 (5 if pellets too small) consecutive sections were immunostained using a rabbit antiserum raised against reptarenavirus NP and DAB as chromogen, with haematoxylin counterstain. The figure shows box-plots overlaid with scatter plots of the percentages of NP-positive cell area/section determined by QuP or UNet and cells/section determined by QuP+C (Y-axis, logarithmic scale) for freshly UGV-1 inoculated cells (UGV-1) or cells passed at 15 d post UGV-1 inoculation (UGV-1 P1) at the different temperatures (X-axis), at D3 or D6 sampling timepoints. The graphs depict the statistical significant differences on NP expression among different temperatures: *: $0.05 \geq p\text{-value} > 0.01$; **: $0.01 \geq p\text{-value} > 0.001$; ***: $p\text{-value} < 0.001$. The raw data are provided in Table S5. The statistical analyses are also presented in Table S4.

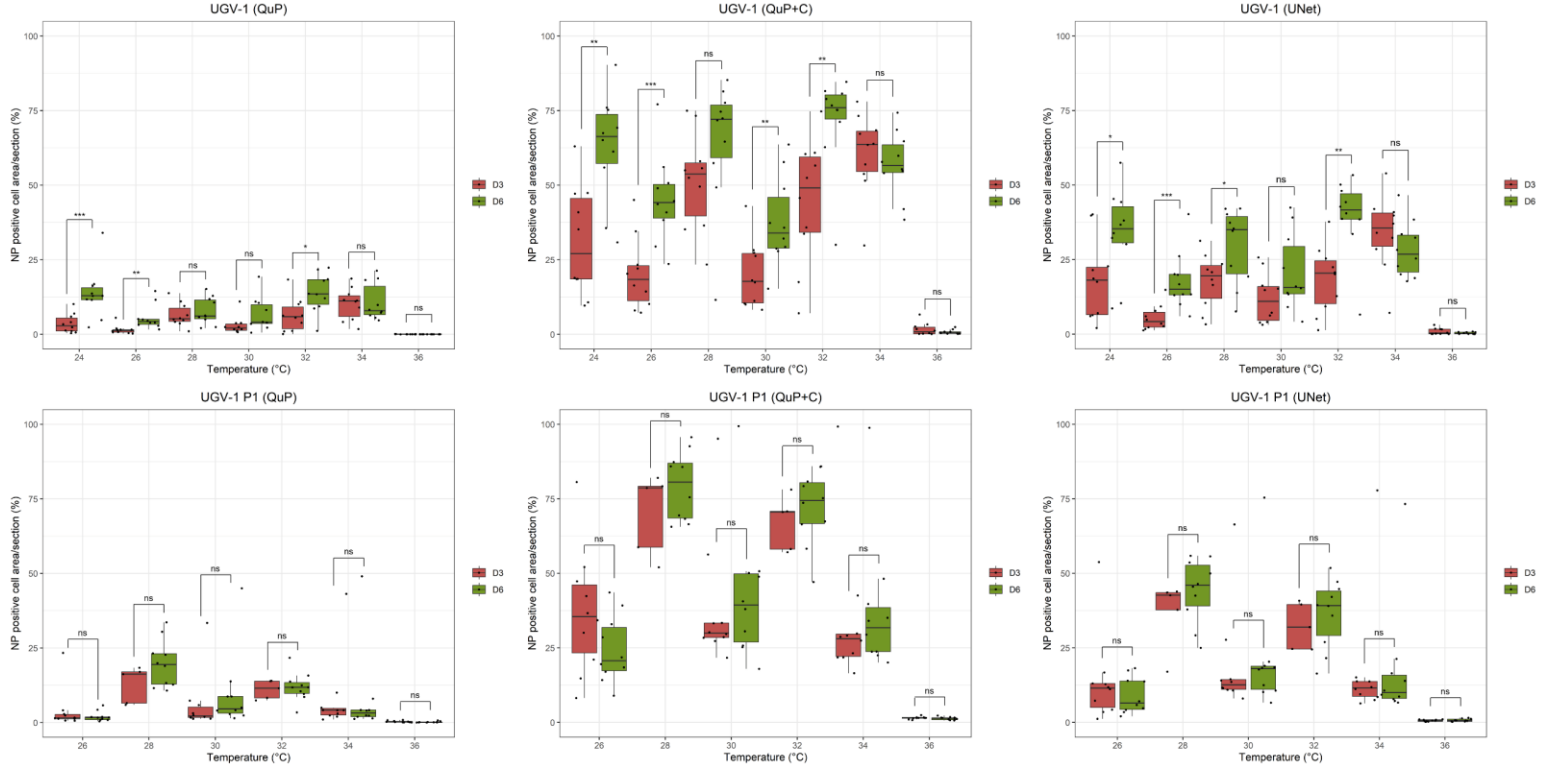


Figure S13. Statistical analyses on the quantification of NP expression in I/1Ki cells infected with UGV-1 comparing different timepoints for each temperature. Cell pellets were prepared, formalin-fixed and paraffin-embedded. For each pellet, 10 (5 if pellets too small) consecutive sections were immunostained using a rabbit antiserum raised against reptarenavirus NP and DAB as chromogen, with haematoxylin counterstain. The figure shows box-plots overlaid with scatter plots of the percentages of NP-positive cell area/section determined by QuP or UNet and cells/section determined by QuP+C (Y-axis, logarithmic scale) for freshly UGV-1 inoculated cells (UGV-1) or cells passaged at 15 d post UGV-1 inoculation (UGV-1 P1) at the different temperatures and timepoints (X-axis). The graphs depict the statistical significant differences on NP expression between D3 and D6 timepoints for each temperature: *: $0.05 \geq p\text{-value} > 0.01$; **: $0.01 \geq p\text{-value} > 0.001$; ***: $p\text{-value} < 0.001$; ns: not significant. The raw data are provided in Table S5. The statistical analyses are also presented in Table S4.

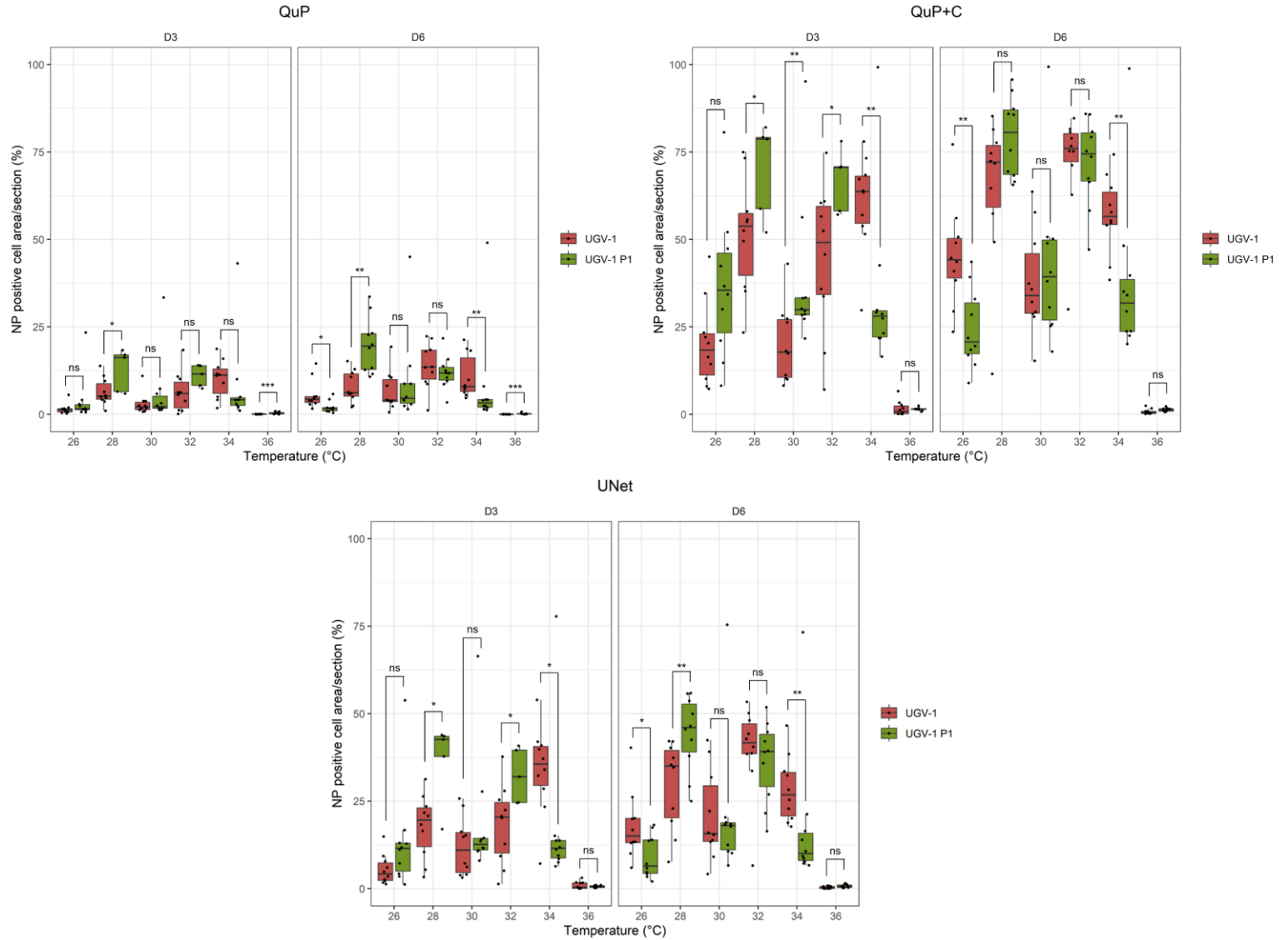


Figure S14. Statistical analyses on the quantification of NP expression comparing freshly and passaged UGV-1 infected I/1Ki cells for each timepoint and temperature. Cell pellets were prepared, formalin-fixed and paraffin-embedded. For each pellet, 10 (5 if pellets too small) consecutive sections were immunostained using a rabbit antiserum raised against reptarenavirus NP and DAB as chromogen, with haematoxylin counterstain. The figure shows box-plots overlaid with scatter plots of the percentages of NP-positive cell area/section determined by QuP or UNet and cells/section determined by QuP+C (Y-axis, logarithmic scale) for freshly UGV-1 inoculated cells (UGV-1) or cells passaged at 15 d post UGV-1 inoculation (UGV-1 P1) at the different temperatures and timepoints (X-axis). The graphs depict the statistical significant differences on NP expression between freshly and passaged infected cells: *: $0.05 \geq p\text{-value} > 0.01$; **: $0.01 \geq p\text{-value} > 0.001$; ***: $p\text{-value} < 0.001$; ns: not significant. The data at 24°C, which are available only for the freshly UGV-1 inoculated cells (see Figures 4, S12 and S13), are not shown. The raw data are provided in Table S5. The statistical analyses are also presented in Table S4.

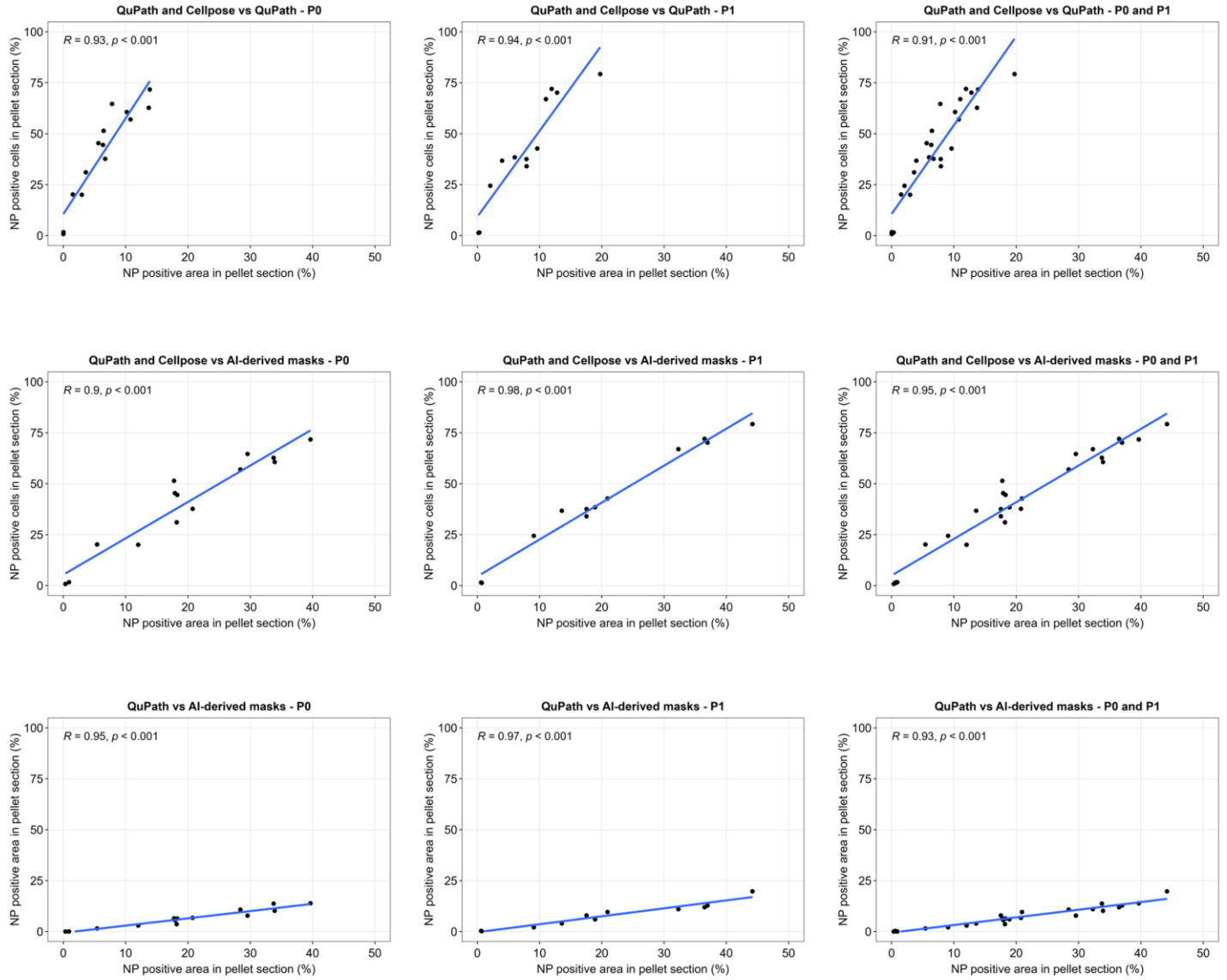


Figure S15. NP expression positive correlation in the comparisons of the different quantification methods. We calculated the Spearman's rank correlation coefficient (R) for the pairwise comparisons among the percentage of NP positive cell area/section determined via QuP or UNet and the percentage of NP positive cells/section determined via QuP+C. For each comparison cells freshly inoculated with UGV-1 (UGV-1) and passaged 15 d post UGV-1 inoculation (UGV-1 P1) were analysed either together or separately. The R and p -values (p) are shown with the respective graphs and in Figure S16.

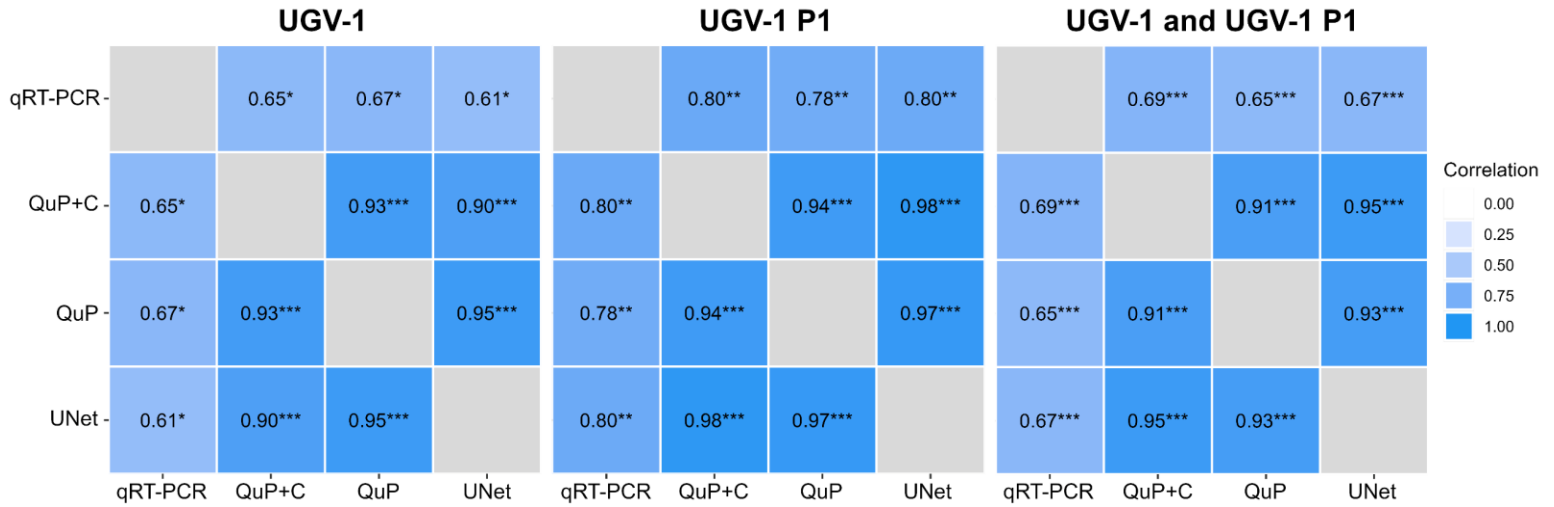


Figure S16. Correlation matrixes of comparisons among virus RNA release and the NP expression quantification methods. Correlation matrixes report the Spearman's rank correlation coefficients (R) and the levels of significance for the pairwise comparisons among the amount of virus RNA release/cell, the percentage of NP positive cell area/section determined via QuP or UNet, and the percentage of NP positive cells/section determined via QuP+C. For each comparison cells freshly inoculated with UGV-1 (UGV-1) or passaged 15 d post UGV-1 inoculation (UGV-1 P1) were analysed either together or separately. Levels of significance: *: $0.05 \geq p\text{-value} > 0.01$; **: $0.01 \geq p\text{-value} > 0.001$; ***: $p\text{-value} < 0.001$. The respective graphs are shown in Figures 5 and S15.

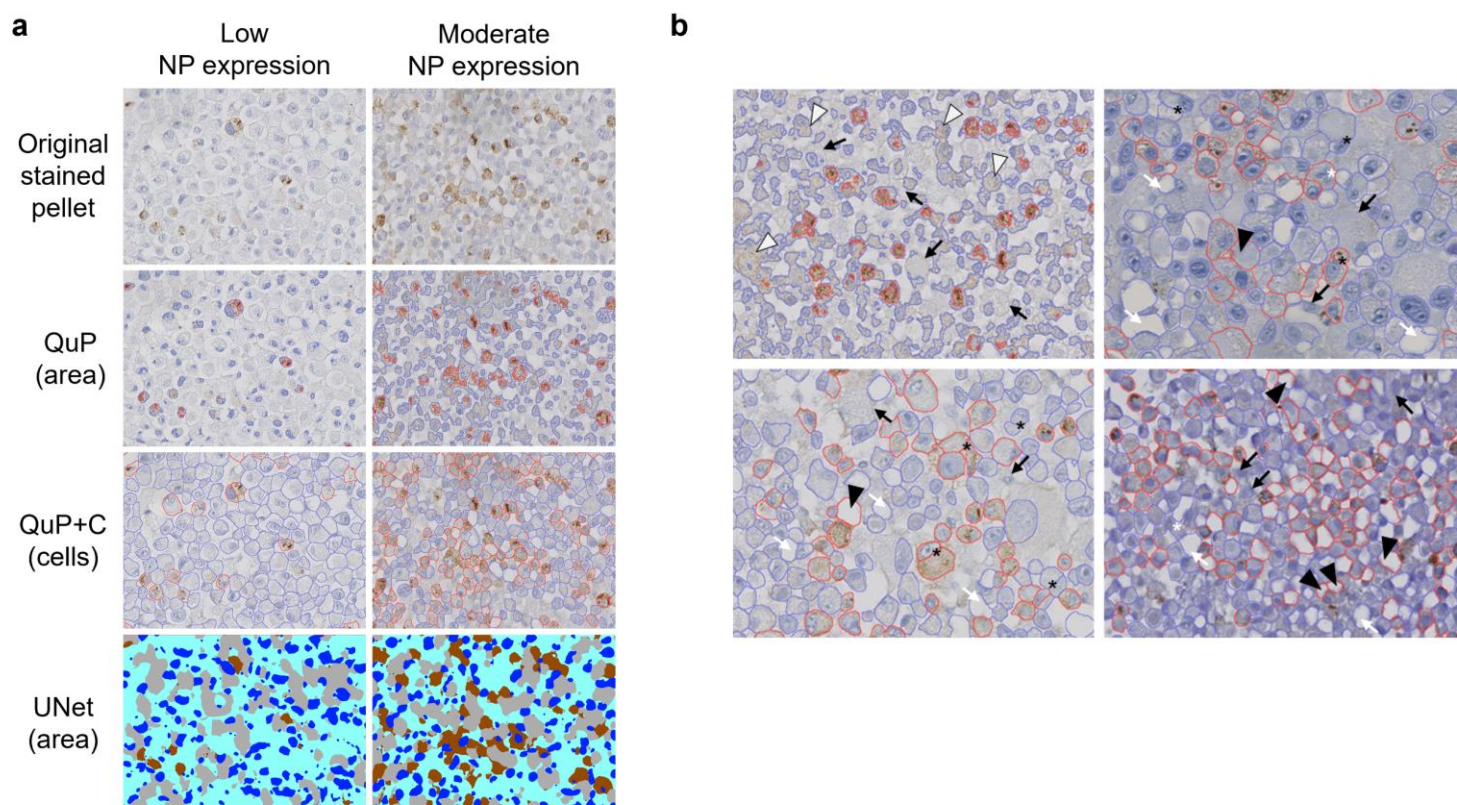


Figure S17. Illustration of challenges by QuP, QuP+C and UNet for the quantification of NP expression. Cell pellets were prepared, formalin-fixed and paraffin-embedded. For each pellet, consecutive sections were immunostained using a rabbit antiserum raised against reptarenavirus NP and DAB as chromogen, with haematoxylin counterstain. The figure shows examples of segmentation and classification outputs by QuP (NP positive surface: red outline; NP negative surface: blue outline), QuP+C (NP positive cells: red outline; NP negative cells: blue outline) or UNet (NP positive cytoplasm: brown; NP negative cytoplasm: pale blue; nuclei: dark blue; background: gray). **(a)** Pellets with low or moderate NP expression and weak contrast led to poor detection of the negative cytoplasmic area by QuP software, while the cells/cell area segmentation by QuP+C or UNet, respectively, were less affected. The same region of a pellet section is represented in each column and is shown across the three tools; the original pellet image is shown for reference. **(b)** Examples of incorrect segmentation and classification of cell area/cells by QuP (top left) or QuP+C (top right and bottom). Absence of segmentation: black arrow; segmentation of an empty space: white arrow; oversegmentation: black asterisk; undersegmentation: white asterisk. False positive classification: black arrowhead; false negative classification: white arrowhead.